Structural Characterization of the (Methanol)$_4$ Potential Energy Surface

Jorge David,[†] Doris Guerra,[‡] and Albeiro Restrepo*[,‡]

Departamento de Ciencias básicas−Ingeniería Física, Universidad Eafit, AA 3600 Medellín, Colombia, and Grupo de Química-Física Teórica, Instituto de Química, Universidad de Antioquia, AA 1226 Medellín, Colombia

Received: May 3, 2009; Revised Manuscript Received: August 2, 2009

In this paper, we report the geometries and properties of the structural isomers obtained from a random walk of the potential energy surface (PES) of the methanol tetramer. Thirty-three structures were obtained after B3LYP/6-31+g* optimization of 94 candidate structures generated from a stochastic search of the PM3 conformational space. The random search was carried out using a recently proposed modified Metropolis acceptance test in the simulated annealing (SA) procedure. Corrections for the basis set superposition error (BSSE) show improvements on the binding energies of the clusters in an average of ∼2.0 kcal/mol, while geometries are predicted to be less sensitive to BSSE corrections. MP2/aug-cc-pvdz calculations on representative structures did not change the geometries but predicted better binding energies. Highly correlated CCSD(T) energies were calculated on the B3LYP and MP2 stationary points and used to establish relative stabilities. We report several new conformations and group the structures into six distinct geometrical motifs. Only the cyclic tetramers with four primary hydrogen bonds in the same plane are predicted to have significant populations. Secondary hydrogen bonds, those for which the donated proton comes from an alkyl group, lead to a rich conformational space.

1. Introduction

Chemical systems bonded via hydrogen bond networks are the subject of intensive research in many areas of science, ranging from chemistry, physics, and biology to nanotechnology and interstellar chemistry. Networks of hydrogen bonds have a major contribution to the stabilization of secondary and tertiary structures of biopolymers such as proteins and nucleic acids. Solvation processes and chemical reactions are strongly influenced by the presence of hydrogen bonds. A testament to the relevance of the subject of hydrogen-bonded networks is the vast scientific literature devoted to its study. We cite a few very recent developments in the field. LaPointe and co-workers[1] identified three types of networking hydrogen bonds as contributing factors to the stability of α-helical peptides; their quantum theory of atoms in molecules (QTAIM) treatment predicts contributions from N−H···O═C at three and four positions apart as well as from N−H···O═C three positions apart. Water clusters, responsible for the structure and properties of liquid water are also held together via hydrogen bonds. Bates and Tschumper[2] have concluded that high levels of electron correlation with large basis sets are needed to correctly describe the energetics associated with conformational isomers of water hexamers. Similar studies have been reported by Olson et al.,[3] Xantheas et al.,[4] and Dalke and co-workers.[5] Klopper et al.[6] have shown that for the same water hexamers, the correlation energy converges to the CBS limit slowly when correlation-consistent basis sets are used. Olivera and Vasconcellos[7] have shown that in alcohol/water mixtures, water and alcohol molecules interact by simultaneously forming primary and secondary hydrogen bonds. A recent study has shown the pivotal role that hydrogen bonds play in the molecular interactions responsible for the formation of (ethanol)$_2$−water heterotrimers,[8] and such interactions are thought to be of significant relevance in the formation of the ethanol/water azeotrope; on the other hand, it is not well understood how liquid mixtures of methanol/water, capable of forming hydrogen bond networks similar to those in ethanol/water mixtures, do not exhibit an azeotrope and therefore can be separated by distillation. Many aspects concerning hydrogen bonding remain unclear,[9] probably due in part to the difficulties in accurate theoretical treatment of the complex energy decomposition schemes for these interactions.[10] Cooperative polarization[11] and cooperative charge transfer[12−14] have been proposed as the main factors contributing to the stabilization of hydrogen bond networks. Pérez and co-workers have shown that both effects are involved in the formation of stable water tetramers.[15]

A problematic issue in the study of molecular and atomic clusters is the generation of equilibrium structures. Recently,[15−17] a modification of the Metropolis acceptance test in the simulated annealing optimization procedure[18−20] was proposed as means for generating cluster candidate structures that undergo further optimization by traditional gradient-following techniques. The method, incorporated into the ASCEC (after its Spanish acronym annealing simulado con energía cuántica) program,[16] retains the comparative advantages and disadvantages of stochastic optimization over analytical methods,[21] namely, initial guess independence, exhaustive exploration of the potential energy surface, and the ability to jump over energy barriers and to sample several energy wells on the same run without getting trapped in local minima; however, the method is still computationally intensive because of repetitive evaluation of the energy function. The method was successfully applied to the study of the water tetramer[15] and of small neutral and charged lithium clusters,[17] affording contributing new structures never before reported in the literature.

* To whom correspondence should be addressed. E-mail: albeiro@matematicas.udea.edu.co.
[†] Universidad Eafit.
[‡] Universidad de Antioquia.

10.1021/jp9041099 CCC: $40.75
Published on Web 08/27/2009

There is a long and growing list of studies regarding liquid methanol.[22,23] As opposed to water, where the structure of the liquid phase is dominated by hydrophilicity, methanol exhibits both hydrophilic and hydrophobic interactions due to the presence of the OH bonds and the methyl groups, respectively. Only two contributing structures were proposed for the methanol tetramer[24] before the study by Boyd and Boyd,[25] who explored many geometrical possibilities and reported 12 stable structures spread among various geometrical motifs. It seems generally accepted that for small clusters held together via hydrogen bonds (water, methanol, ethanol, etc. and their mixtures, total number of molecules $n < 6$), planar cyclic structures for the hydrogen bond network are the most stable configurations.[8,15,25] Pauling hypothesized that liquid methanol is composed mainly of cyclic hexamers and octamers;[26] recent X-ray spectroscopy and DFT calculations by Kashtanov and co-workers[27] and by Wilson and co-workers[28] seem to validate Pauling's idea, with the exception that chain-like clusters are also observed. Previous studies on methanol clusters and liquid methanol are very well described in the paper by Boyd and Boyd;[25] to summarize their discussion, QM/MM treatments are reported in refs 29 and 30, methanol trimer studies are in refs 31 and 32, methanol tetramers are in ref 24, small methanol clusters ($n = 2 - 8$) by B3LYP/6-31+g* are in ref 33, small methanol clusters ($n = 2 - 9$) by Montecarlo simulations are reported in ref 34, classical MD studies in liquid methanol are in ref 35, Montecarlo simulations in liquid methanol are in ref 36, and ab initio MD are in refs 37−39.

In this paper we report a treatment of the methanol tetramer with the ASCEC method described in refs 15 and 17. This work is a contribution to the still limited understanding of the structures of methanol tetramers and of the molecular interactions arising from hydrogen bond networks which drive structural preferences.

2. Computational Methods

We used the molecular cluster capabilities of the ASCEC program, which contains an adapted version of the simulated annealing (SA) optimization algorithm. The annealing algorithm was used to generate candidate structures after a random walk of the PM3[40,41] PES. The hybrid B3LYP density functional[42−44] in conjunction with the 6-31+g* basis set was used to optimize and characterize the structures afforded by ASCEC; the B3LYP/6-31+g* methodology has proven to give very good quality results at a reasonable computational cost in the study of similar hydrogen bond networks.[8] Because several candidate structures converged to the same equilibrium geometry, only a few stationary points were found by this procedure. The located structures were reoptimized at the same B3LYP/6-31+g* level, accounting for the BSSE superposition error[45] by the counterpoise method[46] as implemented in the Gaussian 03 suite of programs.[47] Analytical harmonic second derivative calculations were used to characterize all stationary points as true minima (no negative eigenvalues of the Hessian matrix) or saddle points. To have a better account of electron correlation, the most stable overall structures (group I, see below) as well as the most stable structures from each group were optimized and characterized at the MP2/aug-cc-pvdz level. BSSE corrections were evaluated via single-point calculations on the optimized geometries at the same level. Highly correlated CCSD(T)[48] energies were calculated on all of the located minima and used to predict relative stabilities and populations. Isomer populations, x_i, within a given PES were estimated by[49]

$$x_i = \frac{g_i e^{-E_i/k_B T}}{\sum_i g_i e^{-E_i/k_B T}} \quad (1)$$

where g_i is the degeneracy of isomer i and E_i stands for one of the B3LYP, MP2 Gibbs free energy, or the B3LYP, MP2, CCSD(T)//B3LYP, or CCSD(T)//MP2 electronic energy. Binding energies (BE) were calculated by subtracting four times the energy of the methanol monomer from the energy of the cluster; relative binding energies (ΔBE) were calculated as the difference between the energy of the most stable cluster and the energy of a particular cluster. All optimizations and frequency and energy calculations were carried out using the Gaussian03[47] suite of programs.

3. Results and Discussion

3.1. ASCEC Conditions. We used the big bang approach to construct the initial geometry for the ASCEC run, namely, all methanol molecules were placed at the same position with the same orientation, allowing them to evolve under the annealing conditions within a cube of 8 Å in length. The PM3 semiempirical Hamiltonian was used to calculate the energy of randomly generated cluster configurations. We used a geometrical quenching route with an initial temperature of 500 K, a constant temperature decrease of 10%, and 300 total temperatures. The stochastic sampling generated 94 candidate structures, 83 of them after satisfying the modified Metropolis test ($|\Delta E/E_j| < \exp[-\Delta E/k_B T]$) and the remaining 11 after a random move resulted in lowering the energy.

3.2. Cluster Structures. The B3LYP and MP2 equilibrium geometries were produced following the procedure described in the Computational Methods section. All geometry optimizations were carried with no imposition of symmetry constraints as the structures coming from ASCEC are randomly generated and belong to the C_1 point group; however, some of the located stationary points have higher symmetries.

3.2.1. Geometries. We found 33 equilibrium structures in the B3LYP/6-31+g* PES classified into six different geometrical motifs, shown in approximate decreasing order of stability in Figures 1−6. Figure 7 shows the relative stability of the structures and groups; an overlap between motifs due to the many geometrical possibilities is observed. Our classification is arbitrary as chains and other patterns fit in our groups; also, some structures could belong to more than one group because several motifs may be present in the same cluster. We have declined to name the 33 structures using conventional descriptive methods because for such a large set of isomers, it may lead to confusion; instead, the six groups are described by the common features of the structures within. We have named the structures by two criteria, global relative stability (1, 2, ..., 33; 1 being the most stable) and relative stability within each group (I_a, I_b, ..., VI_c; I_a being the most stable in group I, etc.). There are plenty of possibilities and probably more structures to be found within each group due to the orientations of the H and CH_3 substituents relative to the geometrical pattern defining the group. Calculations accounting for the BSSE did not change the landscape of the $(methanol)_4$ PES as the same structures were located with negligible geometry distortions.

Brief Description of the Groups. Group I contains the three most stable structures. The geometrical pattern defining the group is a planar network of four primary hydrogen bonds with the methyl groups located above and under the plane. No secondary bonds are present in this group. Group II is character-

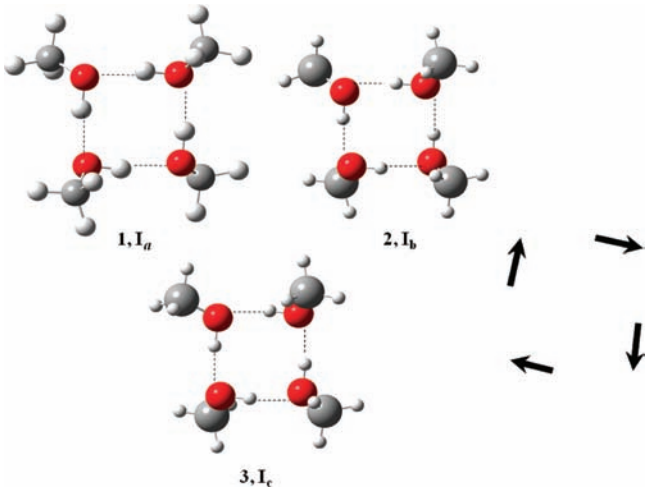

Figure 1. Group I. Stabilization due to cooperative polarization. The arrangement of in-plane dipole moment components is shown.

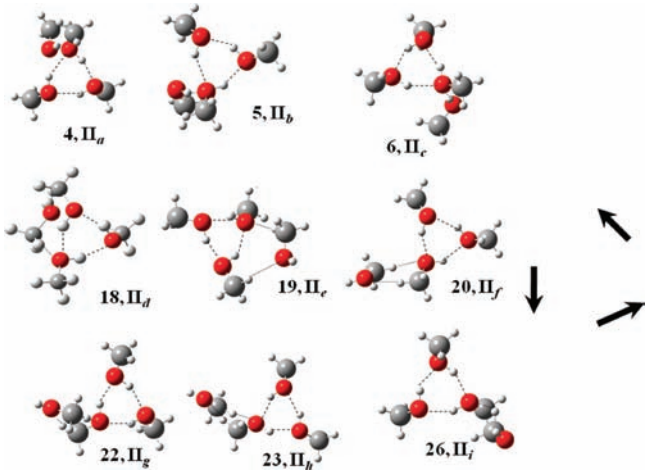

Figure 2. Group II. The arrangement of in-plane dipole moment components is shown.

ized by a planar network of three primary hydrogen bonds (a trimer) interacting with an extra methanol molecule. There are a total of nine structures in this group. Group III exhibits a five-sided ring in which the four methanol molecules contribute; there are one secondary and three primary hydrogen bonds in the ring, and the fifth side is afforded by a C−O bond in one of the methanol molecules, which is the one always contributing with the secondary bond and always leaving its own OH hydrogen free from cluster bonding. We located five structures in this group. The 10 structures located in group IV display a four-sided cyclic pattern with contributions from three molecules; the cycle contains one secondary and two primary hydrogen bonds in addition to one C−O bond (again, one single molecule affording the secondary bond, the C−O bond, and leaving its own OH hydrogen free from cluster interactions). Group V is defined by a five-sided ring with contributions from three different molecules; the ring features one primary and two secondary hydrogen bonds as well as two C−O bonds; two of the molecules contribute with one secondary bond and one C−O bond each, leaving their respective OH hydrogens free of interactions or used to bond with the fourth methanol. There are three structures in this group. Group VI features a six-membered ring with alternating C−O, primary, and secondary hydrogen bonds; there are always two OH hydrogens not participating in the stabilizing network. There are three structures in this group.

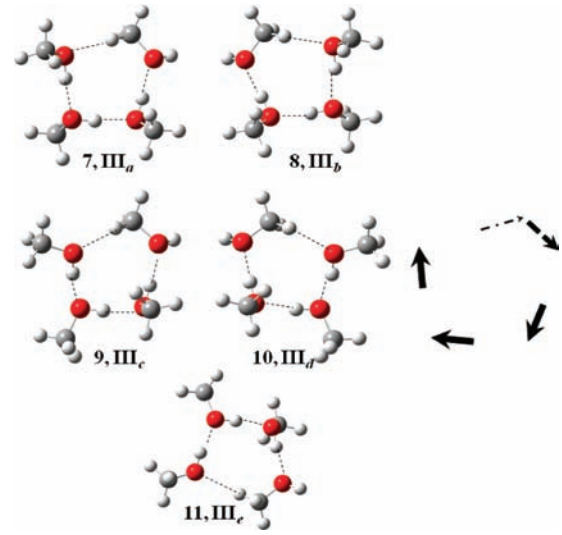

Figure 3. Group III. The defining geometrical motif includes three consecutive primary hydrogen bonds (thick arrows), a secondary hydrogen bond (thin dashed/pointed arrow), and a formal C−O bond (medium thickness, dashed arrow). Structures 7, 8 and 9, 10 are enantiomer pairs. The motif is not always planar.

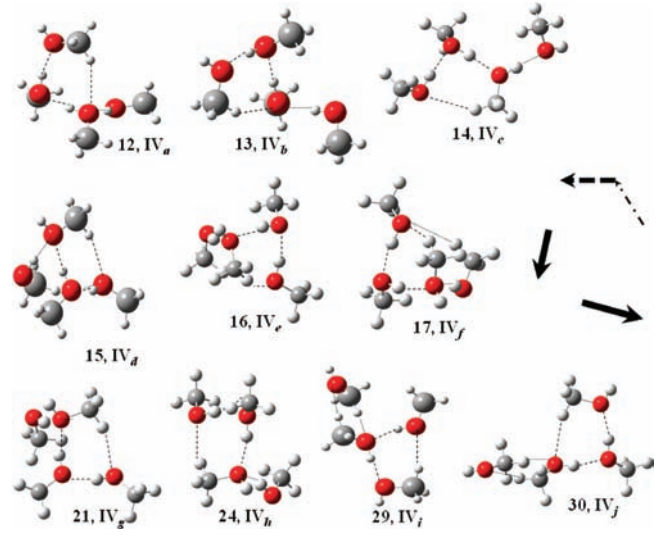

Figure 4. Group IV. The defining geometrical motif includes two consecutive primary hydrogen bonds (thick arrows), a secondary hydrogen bond (thin dashed/pointed arrow), and a formal C−O bond (medium thickness, dashed arrow). The motif is not always planar.

Primary hydrogen bonds, secondary hydrogen bonds, or combinations of both are responsible for the bonding to one or more of the molecules defining the geometrical motif in the cases where there is an extra molecule. Except for groups I and II, the defining cycles are often nonplanar. There are many instances of oxygen atoms acting as double acceptors of primary, secondary, or both kinds of hydrogen bonds. Secondary bonds in the clusters are predicted to be ~38% larger on average than primary bonds; the smallest and largest O···H distances in a primary hydrogen bond are, respectively, 1.75 and 2.06 Å (1.84 Å average, $r_{max} - r_{min} = 0.31$ Å), while for secondary bonds, those distances are 2.31 and 3.02 Å (2.54 Å average, $r_{max} - r_{min} = 0.71$ Å; ratio of the averages = 1.38). Plots of the distributions of O···H distances for primary and secondary hydrogen bonds are included in Figure 8. The distribution of O···H distances for primary hydrogen bonds resembles a Gaussian function centered at the average value; the wider range

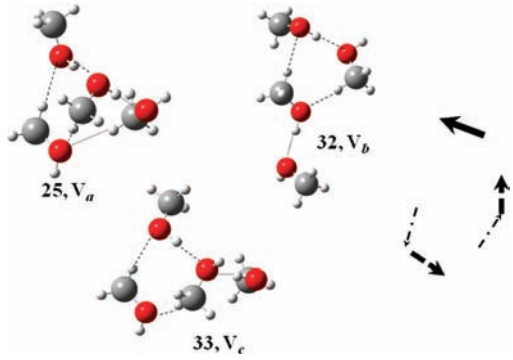

Figure 5. Group V. The defining geometrical motif includes one primary hydrogen bond (thick arrow), two secondary hydrogen bonds (thin dashed/pointed arrows), and two formal C−O bonds (medium thickness, dashed arrows). The motif is not always planar.

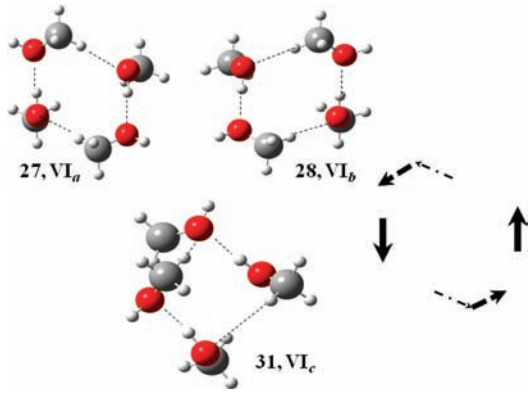

Figure 6. Group VI. The defining geometrical motif includes alternating pairs of primary hydrogen bonds (thick arrows), secondary hydrogen bonds (thin dashed/pointed arrows), and formal C−O bonds (medium thickness, dashed arrows). The motif is not always planar. Structures 27 and 28 are enantiomers.

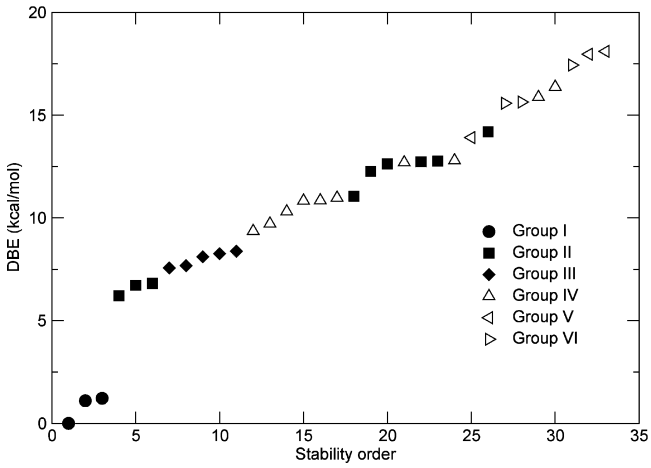

Figure 7. Relative stability of the structural motifs for (methanol)$_4$ clusters. An overlap between groups is observed.

of values for secondary bonds makes for a large variety of possibilities, leading to a rich conformational space.

The rich potential energy surface obtained in this study (33 structures, 6 motifs) is a consequence of the stochastic nature of the search of the quantum conformational space performed by the ASCEC method, which bypasses the structure-guessing step in the search for local minima;[15,17] the diversity of structures is due to the secondary hydrogen bonds, which increase the conformational possibilities (in contrast, water tetramers held together exclusively by primary hydrogen bonds exhibit three

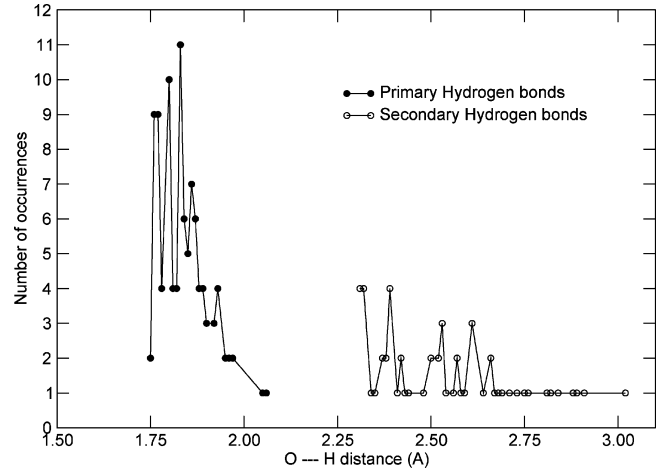

Figure 8. Distribution of the O···H distances for primary and secondary hydrogen bonds in the methanol tetramer.

geometrical motifs and eight structures[15]). The excellent work by Boyd and Boyd,[25] the only previous attempt to systematically characterize the (methanol)$_4$ PES, reported 12 structures distributed among 4 of our groups, the most stable structures and relative stabilities being very similar in both cases (see the section 3.2.2).

A remarkable finding is that despite having no chiral centers, due to the spatial orientation of the entire cluster, we identified several enantiomer pairs, structures 7 and 8, 9 and 10, 27, and 28.

3.2.2. Energies, Cluster Stabilization, and Other Properties. Table 1 classifies the clusters in decreasing order of stability as predicted by the CCSD(T)//B3LYP calculations; Table 1 also shows binding energies (BE) and relative binding energies (ΔBE) at the B3LYP and CCSD(T)//B3LYP levels. Notice the overlap between groups already pointed out and shown in Figure 7. Table 2 shows the same analysis for the selected structures calculated at the MP2/aug-cc-pvdz level. Table 3 lists the unscaled B3LYP ZPE energies, the number of primary and secondary bonds, the average O···H distances in the hydrogen bonds, and the number of OH hydrogens not used in the bonding network. Table 4 shows the isomer populations estimated using eq 1 by different methods on those structures with meaningful contributions.

Generally speaking, Table 1 tells us that the B3LYP and CCSD(T)//B3LYP surfaces are very similar; only minor differences are found in the stability ordering of the less stable isomers. Binding energies are consistently underestimated by ∼10 and ∼8 kcal/mol in the B3LYP and the BSSE-corrected B3LYP surfaces, respectively, when compared with the CCSD(T)//B3LYP calculations; however, the differences in binding energy with respect to the most stable isomer (structure 1) are in excellent agreement. A linear regression produced a remarkable correlation ($R^2 = 0.99$) between the BSSE-corrected and -uncorrected B3LYP binding energies, BE(BSSE) = 1.05 × BE + 1.42. More sophisticated treatment of electron correlation as calculated by the MP2/aug-cc-pvdz and CCSD(T)/aug-cc-pvdz//MP2/aug-cc-pvdz formalisms (Table 2) indicates that accurate binding energies for the open systems studied here are to be calculated only with high levels of electron correlation; however, relative binding energies are not as sensitive. Some qualitative correlations are observed from Table 3. (i) The stability seems to directly depend on the number of primary bonds (structures with four primary bonds are the most stable ones, and structures with two primary bonds are the least stable),

TABLE 1: Energetic Analysis for the (Methanol)$_4$ Clusters[a]

structure	BE[b] kcal/mol	BE(CP)[b,c] kcal/mol	BE[d] kcal/mol	ΔBE[b] kcal/mol	ΔBE(CP)[b,c] kcal/mol	ΔBE[d] kcal/mol
1, I_a	26.89	29.42	37.45	0.00	0.01	0.00
2, I_b	25.86	28.31	36.35	1.03	1.12	1.10
3, I_c	25.76	29.43	36.23	1.13	0.00	1.22
4, II_a	20.05	22.66	31.24	6.84	6.77	6.21
5, II_b	20.00	22.09	30.73	6.89	7.34	6.72
6, II_c	19.48	21.87	29.89	7.41	7.56	7.56
7, III_a	19.82	22.04	29.77	7.07	7.39	7.68
8, III_b	19.82	22.04	29.77	7.07	7.39	7.68
9, III_c	19.05	21.79	29.34	7.84	7.64	8.11
10, III_d	19.08	21.79	29.19	7.81	7.64	8.26
11, III_e	19.13	21.05	29.07	7.76	8.38	8.38
12, IV_a	18.05	19.95	28.09	8.84	9.48	9.36
13, IV_b	18.03	19.92	27.73	8.86	9.51	9.72
14, IV_c	17.82	19.96	27.14	9.07	9.47	10.31
15, IV_d	15.22	17.48	26.61	11.67	11.95	10.84
16, IV_e	15.21	17.74	26.60	11.68	11.69	10.85
17, IV_f	15.10	17.74	26.47	11.79	11.69	10.98
18, II_d	14.15	16.52	26.40	12.74	12.91	11.05
19, II_e	15.51	17.64	25.19	11.38	11.79	12.26
20, II_f	15.33	17.46	24.82	11.56	11.97	12.63
21, IV_g	15.00	17.20	24.75	11.89	12.23	12.70
22, II_g	15.28	17.96	24.72	11.61	11.47	12.73
23, II_h	15.26	17.36	24.68	11.63	12.07	12.77
24, IV_h	14.98	17.62	24.65	11.91	11.81	12.80
25, V_a	13.53	15.45	23.54	13.36	13.98	13.91
26, II_i	14.88	16.59	23.26	12.01	12.84	14.19
27, VI_a	12.54	14.50	21.87	14.35	14.93	15.58
28, VI_b	12.53	14.49	21.81	14.36	14.94	15.64
29, IV_i	12.30	14.39	21.57	14.59	15.04	15.88
30, IV_j	12.24	14.20	21.07	14.65	15.23	16.38
31, VI_c	9.93	11.78	20.01	16.96	17.65	17.44
32, V_b	11.07	12.70	19.48	15.82	16.73	17.87
33, V_c	10.39	12.68	19.34	16.50	16.75	18.11

[a] BE: Binding energy. ΔBE: Relative binding energy. [b] B3LYP/6-31+g*. [c] BSSE corrected by the counterpoise method (BSSE optimized geometries). [d] CCSD(T)/6-31+g*//B3LYP/6-31+g*.

TABLE 2: Energetic Analysis for the (Methanol)$_4$ Clusters[a]

structure	BE[b]kcal/mol	BE(CP)[b,c] kcal/mol	BE[d] kcal/mol	ΔBE[b] kcal/mol	ΔBE(CP)[b,c] kcal/mol	ΔBE[d] kcal/mol
1, I_a	28.65	28.59	32.87	0.00	0.00	0.00
2, I_b	28.02	27.49	32.40	0.63	1.10	0.47
3, I_c	27.86	27.40	32.34	0.79	1.19	0.53
4, II_a	23.65	23.06	28.26	5.05	5.53	4.61
7, III_a	22.88	22.15	26.90	5.77	6.44	5.97
12, IV_a	22.81	21.62	27.01	5.84	6.97	5.86
25, V_a	18.35	17.12	22.17	10.30	11.49	10.70
27, VI_a	16.74	15.36	20.44	11.91	13.29	12.43

[a] BE: Binding energy. ΔBE: Relative binding energy. [b] MP2/aug-cc-pvdz. [c] BSSE corrected by the counterpoise method (BSSE single points). [d] CCSD(T)/aug-cc-pvdz//MP2/aug-cc-pvdz.

not on the total number of hydrogen bonds. Structures 4 and 5, despite exhibiting an extra secondary bond, are less stable than structures 1, 2, and 3; on the other hand, structure 6, with the same number of primary bonds and no secondary bonds, is even less stable. This trend is due to the geometry of the stabilizing network of hydrogen bonds as structures 1, 2, and 3 belong to group I while structures 4, 5, and 6 belong to group II (more on the stabilizing effects below). (ii) The stability ordering of the groups might be correlated with the geometry of the cluster as rings (group I) > rings + extra molecules (group II) > mixed rings (groups III, IV, V, and VI), where mixed rings are cycles having primary and secondary hydrogen bonds as well as formal C−O bonds (some may also be considered as chains); within rings, the ones having the larger number of consecutive primary bonds are the most stable.

Cluster stabilization can be understood by the joint effect of cooperative polarization and cooperative charge transfer, which in turn reinforces cooperative polarization. Figures 1−6 show the cooperative polarization of the methanol dipole moment components that stabilize the clusters; the cooperative effect may include contributions from dipole moment components along the O−H and C−H bonds participating in primary and secondary hydrogen bonds, respectively, as well as components from formal C−O bonds. The geometric arrangement of the components is strongly stabilizing from the electrostatic point of view; group I exhibits a planar octapole (or equivalently, two reinforcing quadrupoles or four reinforcing dipoles) kind of configuration, making it the most stable motif; group II comprises three in-plane components; the other groups show various distortions from the octapole and quadrupoles and from planarity, the more deviated ones being the more unstable. Figure 9 shows the distribution of charges in the participating hydrogen atoms in primary and secondary bonds. Larger amounts of charge transferred, that is, more positive hydrogens,

TABLE 3: Some Properties of the (Methanol)$_4$ Clusters[a]

structure	ZPE[b] kcal/mol	primary bonds	secondary bonds	H left out from OH	$R_{O\cdots H}$[c]	
					primary	secondary
1	134.47	4	0	0	1.76	
2	134.32	4	0	0	1.77	
3	134.28	4	0	0	1.77	
4	134.00	4	1	0	1.89	2.66
5	133.88	4	1	0	1.89	2.71
6	133.98	4	0	0	1.88	
7	133.61	3	1	1	1.79	2.31
8	133.61	3	1	1	1.79	2.31
9	133.58	3	1	1	1.80	2.38
10	133.54	3	1	1	1.80	2.38
11	133.52	3	1	1	1.80	2.38
12	133.43	3	2	1	1.89	2.42
13	133.35	3	1	1	1.81	2.84
14	133.39	3	1	1	1.81	2.88
15	133.59	3	3	1	1.91	2.62
16	133.55	3	3	1	1.91	2.61
17	133.52	3	3	1	1.91	2.65
18	133.60	3	3	1	1.88	2.59
19	133.35	3	2	1	1.88	2.51
20	133.38	3	2	1	1.87	2.54
21	133.37	3	1	1	1.89	2.42
22	133.35	3	2	1	1.88	2.59
23	133.32	3	2	1	1.87	2.55
24	133.34	3	1	1	1.89	2.39
25	132.95	2	3	2	1.81	2.52
26	132.88	3	0	1	1.87	
27	132.81	2	2	2	1.85	2.32
28	132.81	2	2	2	1.85	2.32
29	132.70	2	3	2	1.84	2.50
30	132.64	2	3	1	1.84	2.54
31	132.78	2	4	1	1.92	2.73
32	132.49	2	2	2	1.88	2.47
33	132.58	2	2	2	1.91	2.38

[a] Calculations at the B3LYP/6-31+g* level. [b] Unscaled. [c] Average lengths in Å.

TABLE 4: Isomer Concentrations Estimated by Equation 1 Using Different Methods

structure	B3LYP (%)[a]	B3LYP (%)[b]	MP2 (%)[a]	MP2 (%)[b]	CCSD(T)//B3LYP[a] (%)	CCSD(T)//MP2[a] (%)
1	80	50	63	58	77	54
2	11	20	21	22	12	24
3	9	30	16	20	10	22

[a] Electronic energy only. [b] Using Gibbs free energies at 298.16 K. Only those with significant populations are listed. All B3LYP-related calculations are with the 6-31+g* basis set; all MP2 related calculations are with the aug-cc-pvdz basis set.

which in turn increase the component of the dipole moment along the bond, have larger contributions to the stabilizing effect. Finally, there is a statistical linear relationship between the stability of the clusters and their unscaled B3LYP/6-31+g* ZPE energies, as seen in Figure 10.

4. Conclusions and Perspectives

We report the geometries and properties of 33 structural isomers located in the B3LYP/6-31+g* PES of (methanol)$_4$. The structures were found after a random walk of the PM3 PES subject to a modified Metropolis acceptance test produced 94 candidates. The isomers are divided among six geometrical motifs. We suggest that stabilization comes from both cooperative polarization and cooperative charge transfer. The cooperative polarization arises from the spatial arrangement of the methanol dipole moment components along OH, CH, and CO bonds, producing electrostatically favorable configurations. Only those structures lying typically ~1 kcal/mol above the global minimum are predicted to have meaningful contributions. Binding energies are consistently underestimated by ~10 and ~8 kcal/mol in the B3LYP and the BSSE-corrected B3LYP surfaces, respectively, when compared with the CCSD(T)//

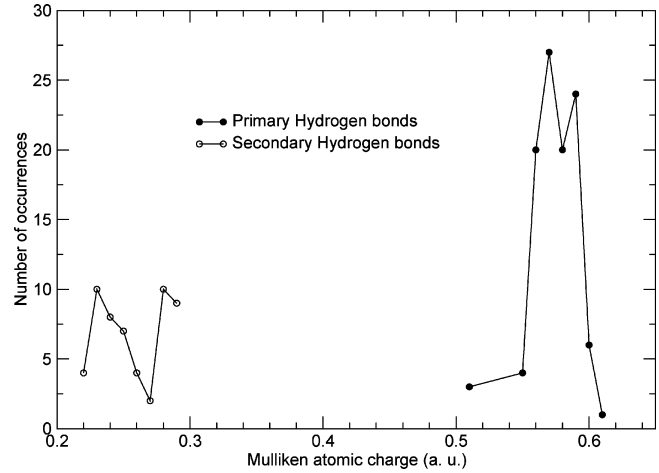

Figure 9. Distribution of atomic charges on hydrogen atoms involved in hydrogen bonding.

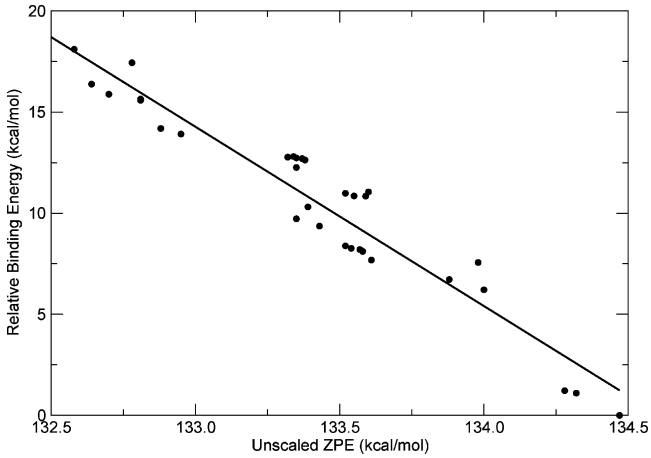

Figure 10. Relative binding energy (kcal/mol) dependence on the unscaled ZPE energy (kcal/mol) for the (methanol)$_4$ clusters. RBE = 0 is the most stable cluster. Linear fitting ($R^2 = 0.93$); BE = 1193.7 − 8.8677 × ZPE.

B3LYP calculations; however, relative binding energies with respect to the most stable isomer show little differences. The results in this study are by no means conclusive for a complete characterization of the PES as there are probably more structures to be located due to the many conformational possibilities afforded by the presence of secondary hydrogen bonds.

Supporting Information Available: Cartesian coordinates for all optimized geometries reported. This material is available free of charge via the Internet at http://pubs.acs.org.

Acknowledgment. Partial funding for this work by Universidad EAFIT, Internal Project Number 103-000093, is aknowledged. We are thankful to the Instituto de Química and Instituto de Física, Universidad de Antioquia, for ample provisions of computer time. We thank professors José López and Cacier Hadad, Instituto de Química, Universidad de Antioquia, for very helpful discussions about this work.

References and Notes

(1) Lapointe, S.; Farrag, S.; Bohórquez, H.; Boyd, R. *J. Phys. Chem. B* **2009**, *113*, 10957.
(2) Bates, D.; Tschumper, G. *J. Phys. Chem. A* **2009**, *113*, 3555.
(3) Olson, R.; Bentz, J.; Kendall, R.; Schmidt, M.; Gordon, M. *J. Chem. Theory Comput.* **2007**, *3*, 1312.
(4) Xantheas, S.; Burnham, C.; Harrison, R. *J. Chem. Phys.* **2002**, *116*, 1493.
(5) Dalke, E.; Olson, R.; Leverentz, H.; Truhlar, D. *J. Phys. Chem. A* **2008**, *112*, 3976.
(6) Klopper, W.; Mamby, F.; Ten-no, S.; Valeev, E. *Int. Rev. Phys. Chem.* **2006**, *25*, 427.
(7) Olivera, B.; Vasconcellos, M. *J. Mol. Struct.: THEOCHEM* **2006**, *774*, 83.
(8) Mejía, S.; Espinal, J.; Restrepo, A.; Modragón, F. *J. Phys. Chem. A* **2007**, *111*, 8250.
(9) Masella, M.; Gresh, N.; Flament, J. *J. Chem. Soc.* **1998**, *94*, 2745.
(10) Koch, W.; Holthausen, M. Hydrogen bonds and weakly bound systems. In *A Chemist's Guide to Density Functional Theory*, 2nd ed.; Wiley: New York, 2002.
(11) Chalasinski, G.; Szczesniak, M.; Cieplak, P.; Scheiner, S. *J. Chem. Phys.* **1991**, *94*, 2873.
(12) Ojamäe, L.; Hermannsson, K. *J. Phys. Chem.* **1994**, *98*, 4271.
(13) Masella, M.; Flament, J. *J. Chem. Phys.* **1998**, *108*, 7141.
(14) King, B.; Weinhold, F. *J. Chem. Phys.* **1995**, *103*, 333.
(15) Pérez, J.; Hadad, C.; Restrepo, A. *Int. J. Quantum Chem.* **2008**, *108*, 1653.
(16) Perez, J. F.; Restrepo, A. *ASCEC V-02: Annealing Simulado Con Energía Cuántica. Property, development and implementation*; Grupo de Química-Física Teórica, Instituto de Química, Universidad de Antioquia: Medellín, Colombia, 2008.
(17) Pérez, J.; Flórez, E.; Hadad, C.; Fuentealba, P.; Restrepo, A. *J. Phys. Chem. A* **2008**, *112*, 5749.
(18) Metropolis, N.; Rosenbluth, A.; Rosenbluth, M.; Teller, A.; Teller, E. *J. Chem. Phys.* **1953**, *21*, 1087.
(19) Kirkpatrick, S.; Gellat, C.; Vecchi, M. *Science* **1983**, *220*, 671.
(20) Aarts, E.; Laarhoven, H. *Simulated Annealing: Theory and Applications*; Springer: New York, 1987.
(21) Restrepo, A.; Mari, F.; Gonzalez, C.; Marquez, M. *Química, Actualidad y Futuro* **1995**, *5*, 101.
(22) Ladanyi, B.; Skaf, M. *Annu. Rev. Phys. Chem.* **1993**, *44*, 335.
(23) Tsuchida, E.; Kanada, Y.; Tsukada, M. *Chem. Phys. Lett.* **1999**, *311*, 236.
(24) Vener, M.; Sauer, J. *J. Chem. Phys.* **2001**, *114*, 2623.
(25) Boyd, S.; Boyd, R. *J. Chem. Theory Comput.* **2007**, *3*, 54.
(26) *Linus Pauling: The Nature of the Chemical Bonds*; Cornell University Press: Ithaca, NY, 1960.
(27) Kashtanov, S.; Augustson, A.; Rubensson, J.; Nordgren, J.; Ågren, H.; Guo, J.; Luo, Y. *Phys. Rev. B* **2005**, *em 71*, 104205.
(28) Wilson, K.; Cavalleri, M.; Rude, B.; Schaller, R.; Catalano, T.; Nilsson, A.; Saykally, R.; Petersson, L. *J. Phys. Chem. B* **2005**, *109*, 10194.
(29) Martin, M.; Sánchez, M.; Olivares del Valle, F.; Aguilar, M. *J. Chem. Phys.* **2002**, *116*, 1613.
(30) Morrone, J.; Tuckerman, M. *Chem. Phys. Lett.* **2003**, *370*, 406.
(31) Mó, O.; Yáñez, M.; Elguero, J. *J. Chem. Phys.* **1997**, *107*, 3592.
(32) Mandado, M.; Grana, A.; Mosquera, R. *Chem. Phys. Lett.* **2003**, *381*, 22.
(33) Ludwig, R. *ChemPhysChem* **2005**, *6*, 1369.
(34) El-Shall, M.; Wright, D.; Ibrahim, Y.; Mahmoud, H. *J. Phys. Chem. A* **2003**, *107*, 5933.
(35) Haughney, M.; Ferrario, M.; McDonald, I. *J. Phys. Chem.* **1987**, *91*, 4934.
(36) Jorgensen, W. *J. Am. Chem. Soc.* **1981**, *103*, 341.
(37) Handgraaf, J.; van Erp, T.; Meijer, E. *Chem. Phys. Lett.* **2003**, *367*, 617.
(38) Morrone, J.; Tuckerman, M. *J. Chem. Phys.* **2002**, *117*, 4403.
(39) Pagliai, M.; Cardini, G.; Righini, R.; Schettino, V. *J. Chem. Phys.* **2003**, *119*, 6655.
(40) Stewart, J. *J. Comput. Chem.* **1989**, *10*, 209.
(41) Stewart, J. *J. Comput. Chem.* **1989**, *10*, 221.
(42) Stephens, P.; Devlin, J.; Chabalowski, C.; Frisch, M. *J. Phys. Chem.* **1994**, *98*, 11623.
(43) Lee, C.; Yang, W.; Parr, R. *Phys. Rev. B* **1988**, *37*, 785.
(44) Becke, A. *J. Chem. Phys.* **1993**, *98*, 5648.
(45) Liu, B.; McLean, A. *J. Chem. Phys.* **1973**, *59*, 4557.
(46) Boys, S.; Bernardi, F. *Mol. Phys.* **1970**, *19*, 553.
(47) Frisch, M. J.; Trucks, G. W.; Schlegel, H. B.; Scuseria, G. E.; Robb, M. A.; Cheeseman, J. R.; Montgomery, J. A., Jr.; Vreven, T.; Kudin, K. N.; Burant, J. C.; Millam, J. M.; Iyengar, S. S.; Tomasi, J.; Barone, V.; Mennucci, B.; Cossi, M.; Scalmani, G.; Rega, N.; Petersson, G. A.; Nakatsuji, H.; Hada, M.; Ehara, M.; Toyota, K.; Fukuda, R.; Hasegawa, J.; Ishida, M.; Nakajima, T.; Honda, Y.; Kitao, O.; Nakai, H.; Klene, M.; Li, X.; Knox, J. E.; Hratchian, H. P.; Cross, J. B.; Bakken, V.; Adamo, C.; Jaramillo, J.; Gomperts, R.; Stratmann, R. E.; Yazyev, O.; Austin, A. J.; Cammi, R.; Pomelli, C.; Ochterski, J. W.; Ayala, P. Y.; Morokuma, K.; Voth, G. A.; Salvador, P.; Dannenberg, J. J.; Zakrzewski, V. G.; Dapprich, S.; Daniels, A. D.; Strain, M. C.; Farkas, O.; Malick, D. K.; Rabuck, A. D.; Raghavachari, K.; Foresman, J. B.; Ortiz, J. V.; Cui, Q.; Baboul, A. G.; Clifford, S.; Cioslowski, J.; Stefanov, B. B.; Liu, G.; Liashenko, A.; Piskorz, P.; Komaromi, I.; Martin, R. L.; Fox, D. J.; Keith, T.; Al-Laham, M. A.; Peng, C. Y.; Nanayakkara, A.; Challacombe, M.; Gill, P. M. W.; Johnson, B.; Chen, W.; Wong, M. W.; Gonzalez, C.; Pople, J. A. *Gaussian 03*, revision D.01; Gaussian, Inc.: Wallingford, CT, 2004.
(48) Pople, J.; Head-Gordon, M.; Raghavachari, K. *J. Chem. Phys.* **1987**, *87*, 5968.
(49) Restrepo, A. Ph.D. Thesis, University of Connecticut, 2005.

JP9041099